Bioorganic & Medicinal Chemistry 20 (2012) 2419–2426

Contents lists available at SciVerse ScienceDirect

Bioorganic & Medicinal Chemistry

journal homepage: www.elsevier.com/locate/bmc

1,3-Phenylene bis(ketoacid) derivatives as inhibitors of *Escherichia coli* dihydrodipicolinate synthase

Berin A. Boughton [a,b], Lilian Hor [a,b], Juliet A. Gerrard [c], Craig A. Hutton [a,b,*]

[a] School of Chemistry, The University of Melbourne, VIC 3010, Australia
[b] Bio21 Molecular Science and Biotechnology Institute, The University of Melbourne, VIC 3010, Australia
[c] Biomolecular Interaction Centre and School of Biological Sciences, University of Canterbury, Christchurch, New Zealand

ARTICLE INFO

Article history:
Received 13 December 2011
Revised 17 January 2012
Accepted 26 January 2012
Available online 10 February 2012

Keywords:
Dihydrodipicolinate synthase
Inhibitor
Slow-binding
Slow-tight binding
Mass spectrometry

ABSTRACT

Dihydrodipicolinate synthase is a key enzyme in the lysine biosynthesis pathway that catalyzes the condensation of pyruvate and aspartate semi-aldehyde. A series of phenolic ketoacid derivatives that mimic the proposed enzymatic intermediate were designed as potential inhibitors of this enzyme and were synthesized from simple precursors. The ketoacid derivatives were shown to act as slow and slow-tight binding inhibitors. Mass spectrometric experiments provided further evidence to support the proposed model of inhibition, demonstrating either an encounter complex or a condensation product for the slow and slow-tight binding inhibitors, respectively.

© 2012 Elsevier Ltd. All rights reserved.

1. Introduction

Lysine and its immediate precursor *meso*-diaminopimelate (*meso*-DAP) are essential elements of bacterial peptidoglycan and proteins.[1,2] As the biosynthetic pathway to lysine is only found in plants and bacteria, it has attracted considerable attention as a target for the design and synthesis of novel herbicides and antibiotics.[3–6] The first committed step in the biosynthesis of lysine is the condensation of pyruvate **1** and (*S*)-aspartate semi-aldehyde (ASA, **2**), catalyzed by the enzyme dihydrodipicolinate synthase (DHDPS) (Fig. 1).[7]

The DHDPS-catalyzed reaction is initiated by condensation of pyruvate **1** with an active site lysine residue (Lys161 in *Escherichia coli* DHDPS) forming a Schiff base. Subsequent tautomerization to the enamine **5** and aldol-type reaction with ASA **2** then generates the acyclic enzyme-bound intermediate **6** (Fig. 2). Transimination of the acyclic intermediate **6** yields the cyclic alcohol HTPA **3**, with simultaneous release of the active site lysine residue.

We previously reported preliminary studies exploring a new class of inhibitor based on analogy to the acyclic enzyme-bound intermediate **6**.[8,9] The crystal structure of DHDPS soaked with pyruvate and succinic semi-aldehyde (SAS) shows an enzyme-adduct closely related to **6**, which lacks the amino group (Fig. 3A).[10] The adduct exists in an extended conformation with dihedral angles ranging from 100 to 179°. We hypothesized that (1,3-phenylene)bisketoacid **7** and (2-hydroxy-1,3-phenylene)bisketoacid **8** would mimic the enzyme bound intermediate and would present the ketoacid functional groups in a constrained, extended conformation (Fig. 3B). Thus, we first synthesized the parent bis(ketoacid) **7** and derivatives **11**–**13** (Fig. 3C) and assayed these compounds for inhibition of DHDPS activity.[8] The compounds showed moderate inhibitory activity against DHDPS (Table 1), and prompted further investigation into more functionalized analogues that more closely mimic the structure of the enzyme-bound intermediate **6**; specifically, phenolic analogue **8** incorporating a hydroxyl group to mimic that at C4 of the enzymatic intermediate **6**. Herein we report the synthesis of phenol-containing compounds **8**, **19** and **20** and detailed analysis of the inhibitory activity and mechanism of action of these compounds and their simpler progenitors through kinetic and mass spectrometric analysis.

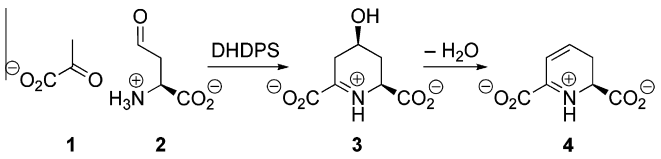

Figure 1. Condensation of pyruvate **1** and ASA **2** to form HTPA **3**, then dehydration to form DHDP **4**.

* Corresponding author. Tel.: +61 3 8344 2393; fax: +61 3 9347 8124.
E-mail address: chutton@unimelb.edu.au (C.A. Hutton).

0968-0896/$ - see front matter © 2012 Elsevier Ltd. All rights reserved.
doi:10.1016/j.bmc.2012.01.045

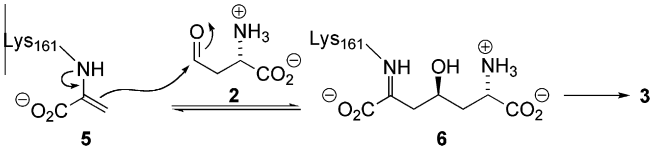

Figure 2. Condensation of pyruvate **1** and ASA **2** to give HTPA **3** proceeds through enamine **5** and enzyme-bound adduct **6**.

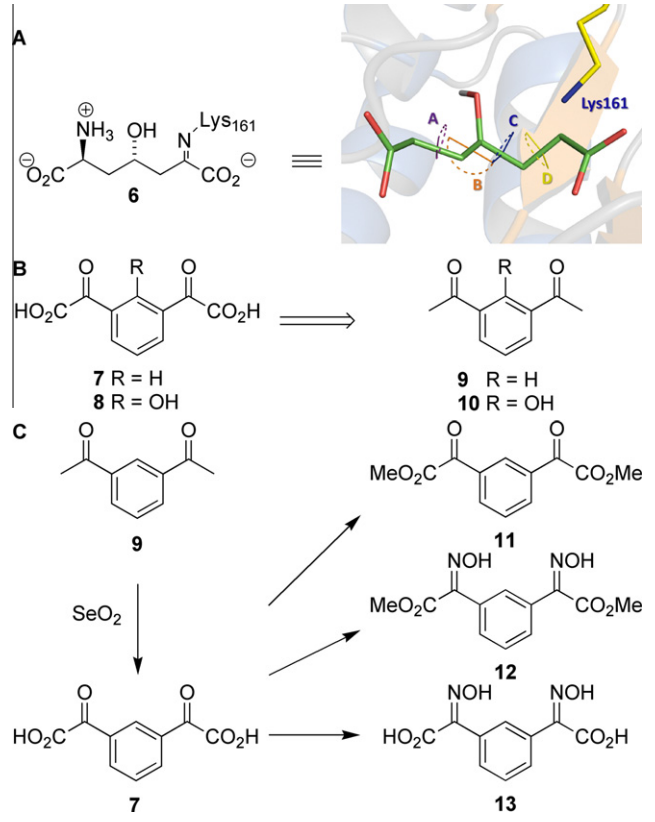

Figure 3. (A) Enzyme tethered intermediate **6** and crystal structure of DHDPS soaked with SAS + pyruvate showing extended structure of analogous condensed adduct. Dihedral bond angles along carbons bonds: $A = 171°$, $B = 179°$, $C = 100°$, $D = 133°$[11]; (B) Retrosynthesis of bis(ketoacid) derivatives **7**, **8** from bis(acetyl)benzene synthons **9**, **10**; (C) Synthesis of bis(ketoacid) **7** and derivatives via oxidation of 1,3-bis-acetylbenzene **9** with SeO_2.[8]

2. Results and discussion

2.1. Synthesis

Our initial strategy toward synthesis of the phenolic bis(ketoacid) **8** was based on analogy to our previously developed

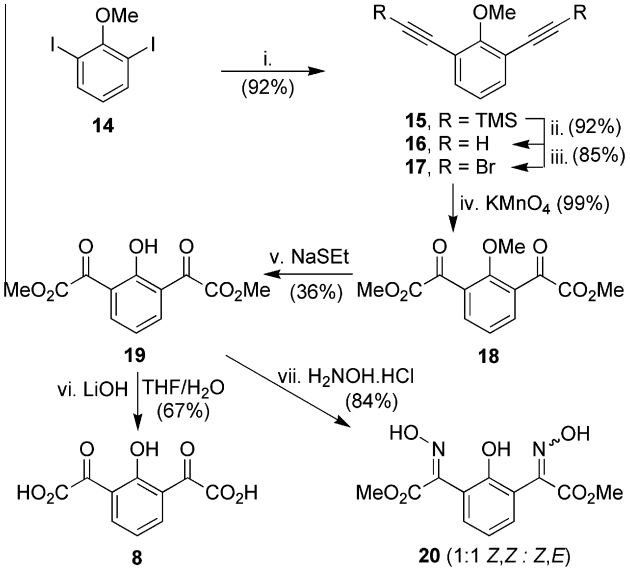

Figure 4. Synthesis of bis(ketoacid)phenol **8**; (i) TMS-acetylene, CuI, Et_3N, 16 h; (ii) KOH, MeOH/H_2O (1:1), 20 min; (iii) NBS, acetone, 3 h; (iv) $NaHCO_3/MgSO_4$, MeOH/H_2O (2:1), $KMnO_4$, 1 h; (v) NaSEt, DMF, 80 °C, 3 h; (vi) LiOH, THF/H_2O (1:1), 3 h; (vii) $H_2NOH{\cdot}HCl$, pyridine, MeOH, 16 h.

synthesis of the model compound **7** in which the ketoacid groups were generated by oxidation of bis(acetyl)benzene **9** (Fig. 3C).[8] Accordingly, we required synthesis of the corresponding 2,6-bis(acetyl)phenol **10**. However, synthetic strategies towards this target were not successful and an alternate strategy was adopted. Li and Liu have reported the transformation of bromoacetylenes into α-ketoesters through treatment with potassium permanganate in aqueous methanol.[12,13] Accordingly, our modified synthetic strategy began by double Sonogashira coupling of diiodoanisole **14** with TMS-acetylene to give bisalkyne **15** in excellent yield (Fig. 4). Silyl-deprotection was effected upon treatment with KOH in aqueous methanol to give the bis-acetylene **16**.[14] Treatment with *N*-bromosuccinimide gave bis(bromoalkyne) **17** in 85% yield.[15] Oxidation of the bromoacetylenes with potassium permanganate in buffered methanol/water then gave the 2,6-bis(ketoester) **18** in quantitative yield.[12,13] Thus, a rapid and high yielding pathway to the core scaffold of the desired bis(ketoacid)phenols was enabled.

Removal of the methyl ether group to unveil the phenol was next investigated. Treatment of **18** with BBr_3, BCl_3 or $AlCl_3$ resulted in only recovery of starting material, or decomposition under forcing conditions. However, treatment of **18** with two equivalents of sodium ethanethiolate in DMF gave the desired phenol **19**, albeit in moderate yield (36%), with recovery of starting material in 10–25% yield.[16–19] Use of one equivalent of the thiolate gave a

Table 1
Inhibition kinetics of phenolic bis(ketoacid) derivatives **8** and **18**–**19**, compared with deoxy-analogues **7** and **11**–**13**[8]

Compound	Screening assay—% inhibition at 5 mM[a]	Time dependent inhibition	Inhibition type
7	49%	K_i^{app} = 2.96 mM	Slow[b]
11	2%	None	N/A
12	15%	K_i^{app} = 0.33 mM	Slow[b]
13	23%	34% at 50 mM, t = 60 min	N/A
18	None	None	N/A
19	10%	K_i^{app} = 12.0 mM K_i^{*app} = 0.04 mM	Slow-tight[c]
8	10%	Estimated K_i^{app} = 11.8 mM K_i^{*app} = 0.29 mM	Slow-tight[c]

[a] Initial screening assays were conducted by incubating DHDPS with inhibitor for 1 min prior to assay.
[b] See Eq. II.
[c] See Eqs. III and IV.

lower yield of the deprotected product, whereas use of greater than two equivalents resulted in the formation of complex mixtures. Presumably, several competing reactions are taking place in which the thiolate reacts at the aromatic ether, the methyl esters, or a combination of both leading to a mixture of demethylated products. Several alternate strategies were tested where the phenol protecting group employed was a benzyl- or *para*-methoxybenzyl-(PMB) ether (see Supplementary data). However, the PMB ether was incompatible with the permanganate oxidation step and poor yields were encountered in the benzyl ether deprotection step. Nevertheless, sufficient material could be produced from methyl ether **18** to facilitate further functional group interconversions. Saponification of the bis(ketoester) **19** gave the corresponding bis(ketoacid) **8** (Fig. 5). Alternatively, treatment of the bis(ketoester) **19** with hydroxylamine hydrochloride in the presence of pyridine provided the bis(oxime)phenol **20**, as a 1:1 mixture of (*Z*,*Z*):(*Z*,*E*) isomers.

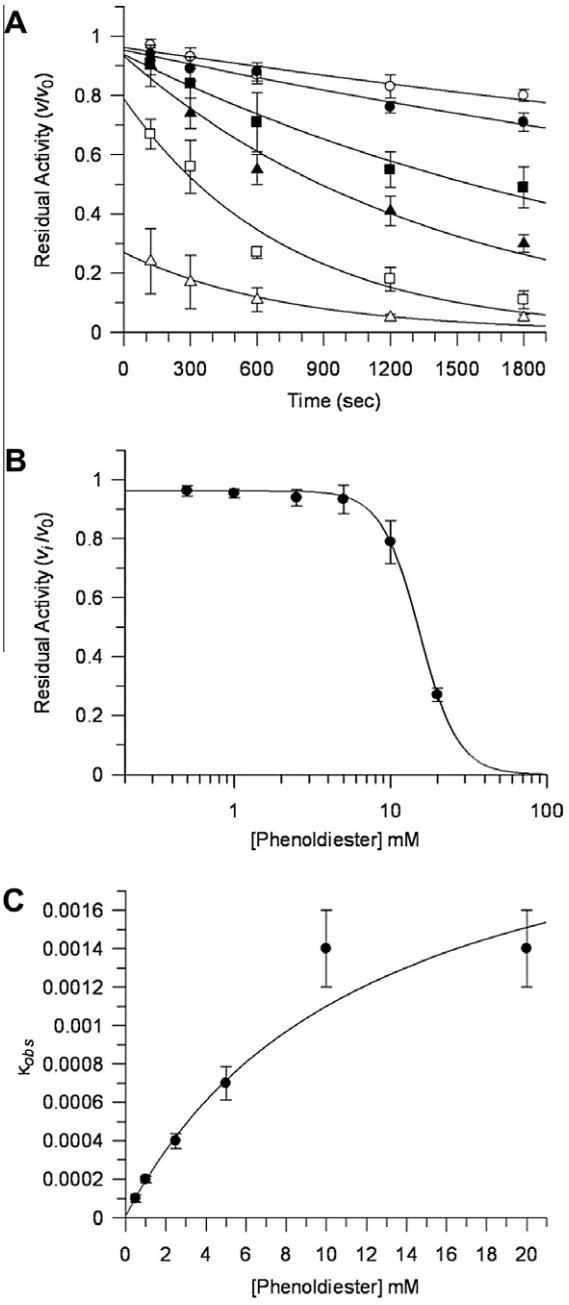

Figure 5. (A) Residual activity of DHDPS upon incubation with bis(ketoester) **19**. [**19**]: ○ = 0.5 mM, ● = 1.0 mM, ■ = 2.5 mM, ▲ = 5.0 mM, □ = 10.0 mM, Δ = 25.0 mM; (B) Estimation of K_i^{app}; (C) Plot of k_{obs} versus [**19**], used to determine K_i^{app}.

2.2. Enzyme inhibition assays

Kinetic assays of DHDPS activity are generally conducted using the 'coupled assay', in which the product of the DHDPS-catalyzed reaction is converted by dihydrodipicolinate reductase (DHDPR) to THDP, with concomitant conversion of NADPH to $NADP^+$, monitored at 340 nm. Analysis of the inhibitory activity of the 2, 6-disubstituted phenols **8** and **18**–**20** against DHDPS was complicated by their high UV absorbances at 340 nm. Accordingly, time-dependent assays were modified to include a serial dilution of a stock solution of DHDPS incubated with inhibitor, prior to addition to substrates.

An initial screen was conducted in which the activity of the enzyme was determined upon treatment with compounds **8** and **18**–**19** at 5 mM. The methyl ether **18** showed no inhibitory activity, whereas the phenols **8** and **19** showed low levels of inhibition at time $t = 0$ (Table 1). Due to production of only small amounts of the separated (*E*,*Z*)- and (*Z*,*Z*)-bis(oxime)phenols **20**, these compounds remain to be tested in kinetic assays. Given that phenols **8** and **19** showed some inhibitory activity and are analogous to the model series demonstrating time dependent inhibition, they were next investigated for time-dependent inhibition.

Though only weak initial inhibition was observed, the bis(ketoester)phenol **19** showed time dependent inhibition, with residual enzyme activity decreasing over time, at all concentrations of inhibitor tested, relative to a control with no inhibitor present (Fig. 5). Interestingly, residual activity curves display decreasing values of v_0 (i.e., *y*-intercept, or residual activity at $t = 0$, <1), suggesting a slow-tight binding mechanism.[20,21] Copeland describes a simple method for estimating K_i^{app}—which represents the initial fast, reversible inhibition—by plotting the values of the *y*-intercepts on a logarithmic scale.[21] A standard isotherm is then fitted to the data and the value of K_i^{app} obtained from the midpoint of the isotherm: using this method the K_i^{app} of **19** was determined to be 15.3 mM. A plot of k_{obs} (rate of inactivation) versus [**19**] (concentration of inhibitor) displays a hyperbolic curve (Fig. 5C), also typical of slow-tight binding.[21] Eq. III allows for accurate determination of K_i^{app} according to the slow-tight binding model. Fitting the data for **19** to Eq. III derived $K_i^{app} = 12.0$ mM, which correlates closely with the estimated value. From Eq. III was also determined the reverse rate, $k_4 = 0.9 \times 10^{-5}\ s^{-1}$. This is consistent with the observation of a small residual rate present after long incubation times (30–60 min). From Eq. IV was determined K_i^{*app}—which represents the slow-tight binding portion of inhibition—which was calculated for **19** to be 0.04 mM.

Analysis of the inhibitory activity of the bis(ketoacid) **8** was performed in the same manner as for bis(ketoester) **19** (Fig. 6). However, the high acidity required an increase in the concentration of buffer used to 500 mM (pH 8.0 at 4 °C HEPES buffer). Compound **8** also had the highest UV absorbance and required two twenty-fold serial dilutions immediately prior to measurement of residual rate. The bis(ketoacid) **8** displays time-dependent inhibition, which was fitted to both irreversible and slow-tight binding modes, with slow-tight binding being a better fit (Fig. 6A).[20,21] Extrapolation of the isotherm generated by plotting the *y*-intercepts versus [**8**] on a logarithmic scale gave an estimated $K_i^{app} = 11.8$ mM (Fig. 6B). Higher concentrations of inhibitor could not be assayed due to its high UV absorbance. The plot of k_{obs} versus [**8**] shows a linear relationship from which it is difficult to differentiate slow binding from slow-tight binding (Fig. 6C). In this case important information from mass spectrometric experiments (see below) demonstrate that **8** forms a covalent adduct with the enzyme, suggesting that

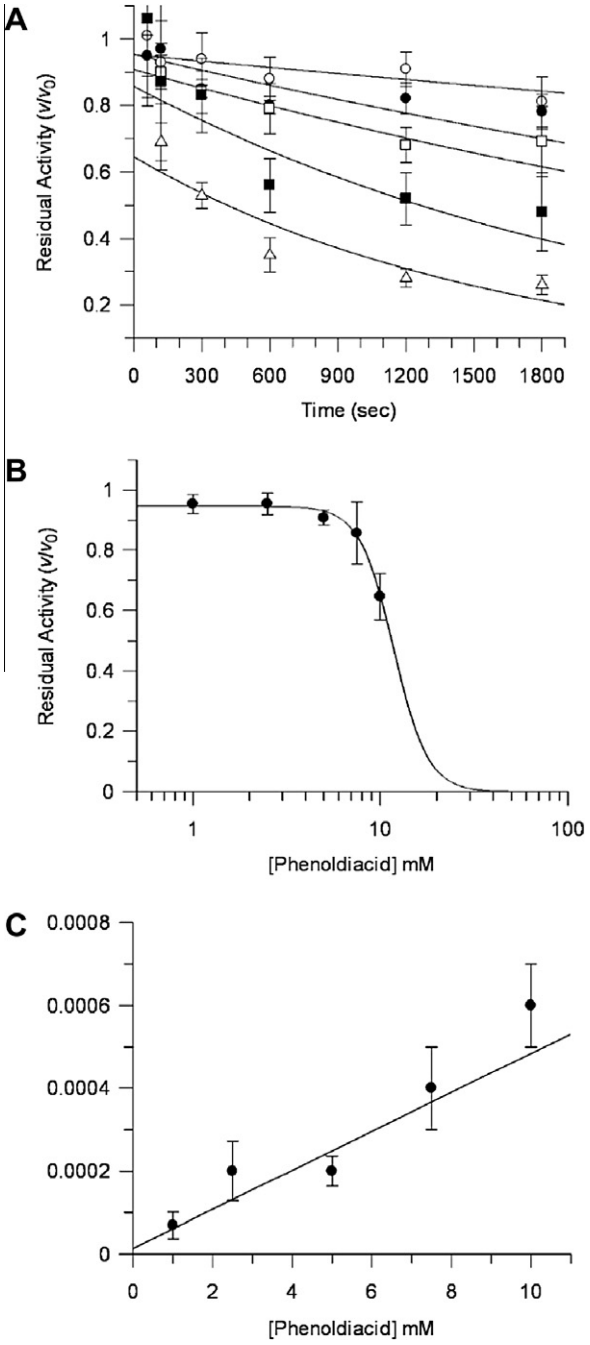

Figure 6. (A) Residual activity of DHDPS upon incubation with bis(ketoacid) **8**. [**8**]: ○ = 1.0 mM, ● = 2.5 mM, □ = 5.0 mM, ■ = 7.5 mM, Δ = 10.0 mM; (B) Estimation of K_i^{app}; (C) Plot of k_{obs} versus [**8**], used to determine K_i^{app}.

the inhibitor is acting in a slow-tight binding manner rather than a slow-binding manner. Fitting the data for **8** to Eq. IV, enables derivation of K_i^{*app} = 0.29 mM.

Substrate protection experiments demonstrate that pyruvate **1** protects the enzyme from inactivation by **8** and **19**, confirming that **8** and **19** are competing with pyruvate for the active site (Fig. 7).

2.3. Mass spectrometric analysis

A slow-tight binding mode of enzyme inhibition generally involves initial binding of the inhibitor followed by 'transition' to a tighter mode of binding, for example by inducing a conformational

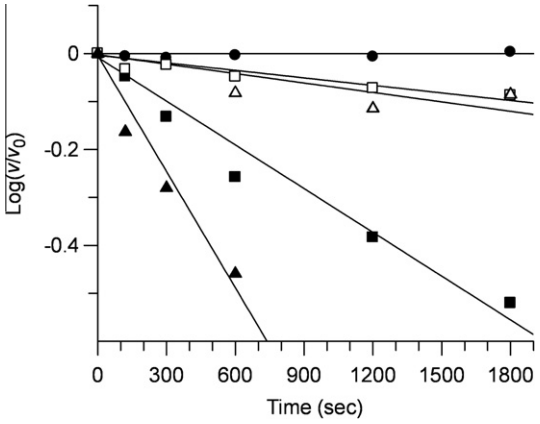

Figure 7. Substrate protection of enzyme inactivation: ● = no inhibitor; ■ = +bis(ketoester)**19**; □ = +bis(ketoester)**19** + 10 mM pyruvate **1**; ▲ = +bis(ketoacid)**8**; Δ = +bis(ketoacid) **8** + 10 mM pyruvate **1**.

change in the enzyme. With identification of a series of compounds that inhibit DHDPS with a slow-tight binding mode, we were interested in exploring the nature of the tight-binding interaction by mass spectrometric studies. The compounds possess α-keto- or α-oximo-esters or acids that could potentially condense with the active site lysine residue in a manner similar to that of the substrate, pyruvate.[22–25] Initial binding would provide an enzyme–inhibitor (or encounter) complex. Nucleophilic addition of the active site lysine ε-amino group into the C=O (or C=N) bond would then generate a tetrahedral hemi-aminal intermediate. Elimination of either water or hydroxylamine from the keto or oxime derivatives, respectively, would lead to formation of an enzyme–inhibitor Schiff-base adduct. Either the hemi-aminal intermediate or Schiff base could potentially represent the tightly bound form of the enzyme–inhibitor adduct. Mass spectrometric analysis was employed to distinguish between these species, with a simple encounter complex expected to show a mass corresponding to [enzyme + inhibitor], whereas a Schiff base adduct would display a lower mass corresponding to the loss of water or hydroxylamine.

Initial investigations of the 1,3-disubstituted benzenes **7**, **12** and **13** demonstrated that they formed simple [enzyme + inhibitor] encounter complexes (Fig. 8). In each case the native enzyme monomer $[M+H]^+$ was the dominant peak in the spectrum. A smaller peak corresponding to $[M+I+H]^+$ was observed.

In marked contrast to the 1,3-disubstituted benzenes, the 2,6-disubstituted phenols **8**, **19** and **20** display a more complex interaction with DHDPS (Fig. 9). The phenolic bis(ketoacid) **8** shows two adducts: a minor encounter complex at *m*/*z* 31509 ($[M+\mathbf{8}+H]^+$) and a predominant condensation product at *m*/*z* 31491 ($[M+\mathbf{8}-H_2O]+H^+$). This result provides support for the assignment of slow-tight binding kinetics to inhibitor **8**. The corresponding bis(ketoester) **19** displays only an encounter complex at *m*/*z* 31537 ($[M+\mathbf{19}+H]^+$), with no condensation product observed. Incubation of DHDPS with bisoxime **20** displays several adducts, with the major species being the condensation product at *m*/*z* 31534 ($[M+\mathbf{20}-NH_2OH]+H^+$). Two other small peaks are present in the mass spectrum; at *m*/*z* 31518, corresponding to DHDPS + 248 amu, corresponding to a species where one of the oximes has condensed with the enzyme and the second oxime group has hydrolyzed to the ketone (i.e., $[M+\mathbf{20}-(2\times H_2NOH)+H_2O]+H^+$). The second, smaller peak at *m*/*z* 31505 is consistent with condensation of **20** with the enzyme and hydrolysis of both esters $[M+\mathbf{20}-H_2NOH-(2\times MeOH)+(2\times H_2O)+H]^+$. Although inhibition by the bisoxime **20** was not subject to kinetic analysis, the mass spectral results suggest that it behaves in a similar manner to the bis(ketoacid) **8** and bis(ketoester) **19**, displaying covalent attachment to the enzyme

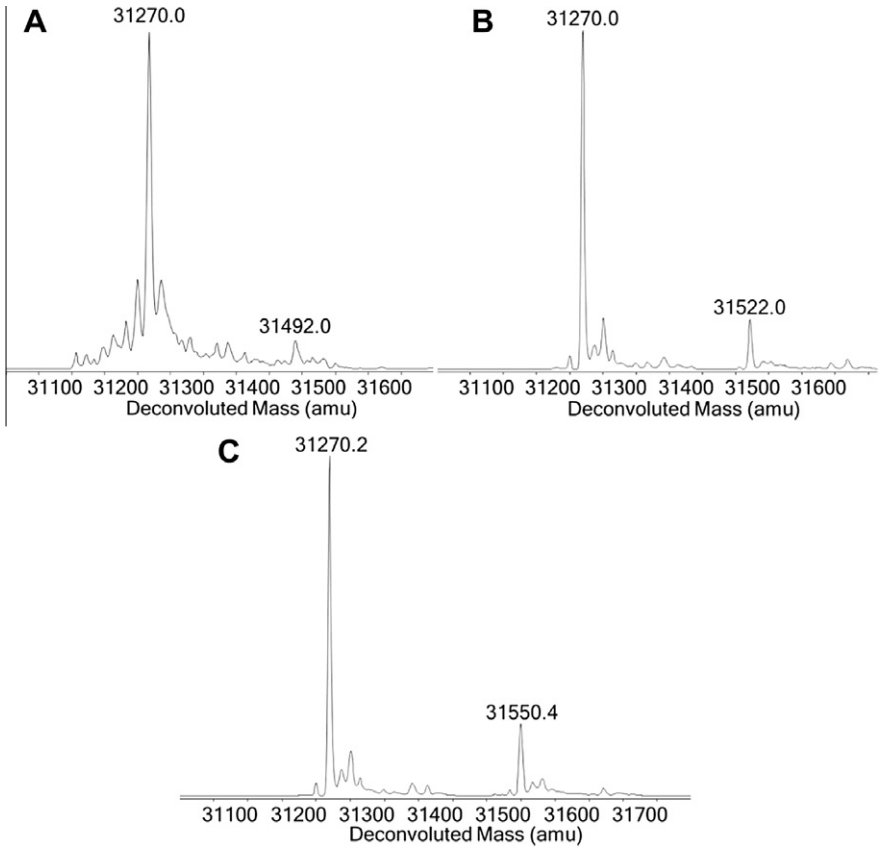

Figure 8. Deconvoluted mass spectra showing native DHDPS = 31270, (A) DHDPS + ketoacid **7** = 31492, (B) DHDPS + oxime acid **13** = 31522, (C) DHDPS + oxime ester **12** = 31550.

and presumably slow-tight binding. Interestingly, these results demonstrate that introduction of the phenolic group promotes condensation with the active site residue, demonstrating the importance of the inclusion of the hydroxyl functionality in order to mimic that at the 4-position of the carbon backbone in enzymatic intermediate **6**.

3. Conclusions

In summary, new constrained bis(ketoacid) and bis(oximino-acid) derivatives have been synthesized and assayed for inhibition of DHDPS. These compounds display time-dependent inhibition and undergo condensation with the enzyme, generating an enzyme-bound adduct that closely resembles the enzymatic intermediate. Kinetic studies show these inhibitors act in a slow-tight binding manner that has not previously been observed for inhibitors of DHDPS. Inclusion of hydroxyl functionality in phenols **8** and **19** in order to better mimic the enzymatic intermediate results in a switch of enzyme inhibition mode to a slow-tight binding model. Mass spectrometric studies support the assignment of slow-tight binding inhibition, through evidence of condensation of the inhibitors with the active site lysine residue.

4. Experimental section

4.1. Materials and methods

Unless otherwise stated, all chemicals were purchased from Sigma–Aldrich or Novabiochem. (see Supplementary data for general experimental procedures).

4.2. Synthetic procedures

4.2.1. 2,6-Bis((trimethylsilyl)ethynyl)anisole (15)

A 3-neck r.b.f. equipped with a nitrogen inlet and seals was flame dried and flushed with nitrogen, then charged with 2,6-diiodoanisole **14** (1.00 g, 2.78 mmol), copper iodide (57.0 mg, 0.29 mmol, 10 mol %), *trans*-dichloro-bis(triphenylphosphine) palladium (101 mg, 0.13 mmol, 4.8 mol %) and triethylamine (25 mL). The reaction flask was flushed with nitrogen for 15 min, then trimethylsilylacetylene (1.9 mL, 12.9 mmol) was added via syringe. The reaction was stirred for 16 h at rt under nitrogen, then was suspended between EtOAc (150 mL) and HCl (1 M, 100 mL). The organic phase was separated then washed with HCl (1 M, 2×75 mL), brine (100 mL), saturated $NaHCO_3$ (100 mL), brine (100 mL), dried ($MgSO_4$), filtered and concentrated in vacuo to give **15** as a pale brown oil (770 mg, 92%). ^{1}H NMR (500 MHz, $CDCl_3$): δ 7.37 (d, 2H, J = 7.9 Hz), 6.95 (t, 1H, J = 7.9 Hz), 4.02 (s, 3H), 0.25 (s, 18H). ^{13}C NMR (125 MHz, $CDCl_3$): δ 162.8, 134.0, 123.2, 117.3, 100.5, 99.2, 60.9, −0.15. υ_{max} (thin film)/cm^{-1} 3073 (w, br), 2959 (w, s), 2899 (w, s), 2846 (w, s), 2153 (m), 1461 (m), 1411 (m), 1248 (m). MS-ESI (*m/z*): $[M+H]^+$ 301.1. MS-EI (*m/z*):300 $[M^{+\cdot}]$, 285 $[M^{+\cdot}-CH_3]$. HRMS-ESI (*m/z*): $[M+H]^+$ calcd for $C_{17}H_{25}OSi_2$ 301.1438; found 301.1437.

4.2.2. 2,6-Diethynylanisole (16)

To a solution of 2,6-bis((trimethylsilyl)ethynyl)anisole **15** (101 mg, 0.335 mmol) in MeOH (20 mL) under nitrogen was added KOH (0.1 M, 7.0 mL, 0.7 mmol, 2.2 equiv). The reaction was stirred for 20 min, then was concentrated in vacuo to half its volume, diluted with HCl (1 M, 20 mL) and extracted with CH_2Cl_2

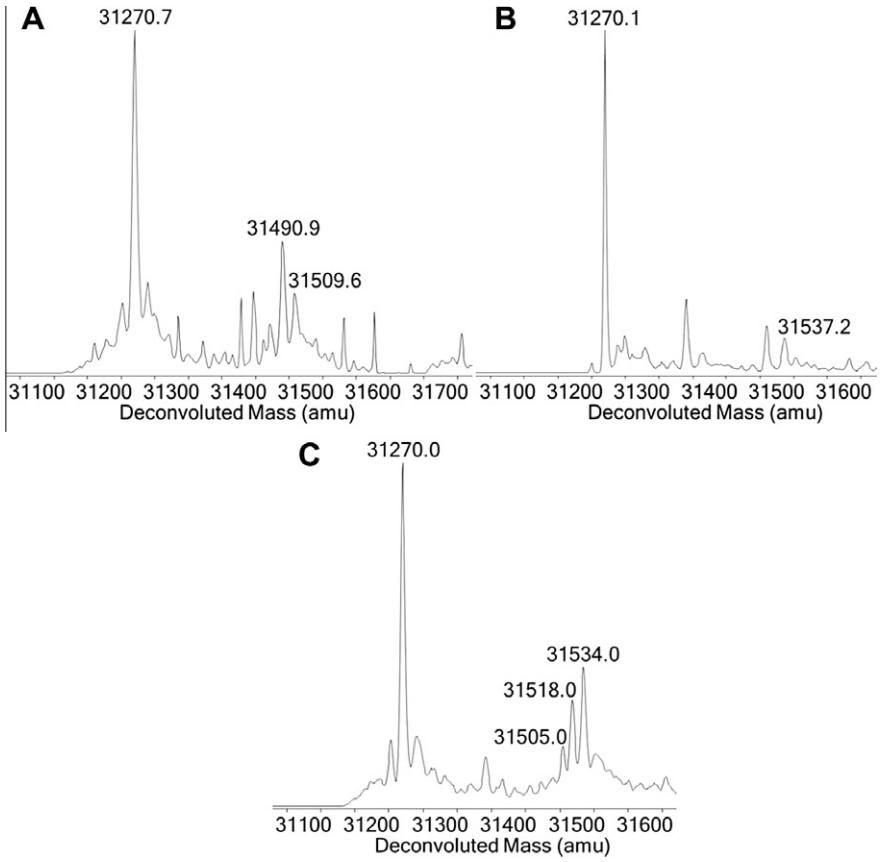

Figure 9. Deconvoluted mass spectra displaying native DHDPS = 31270; (A) DHDPS + bis(ketoacid) **8**—H_2O = 31491, DHDPS + bis(ketoacid) **8** = 31509; (B) DHDPS + bis(keto-ester) **19** = 31537; (C) DHDPS + bis(oxime) **20**—NH_2OH = 31534, and hydrolyzed condensation products at 31505 & 31518.

(3 × 15 mL). The combined organic extracts were dried ($MgSO_4$), filtered, then concentrated in vacuo to give the bis-acetylene **16** as a pale brown oil (48 mg, 92%). ^{1}H NMR (500 MHz, $CDCl_3$): δ 7.46 (d, 2H, J = 7.6 Hz), 7.00 (t, 1H, J = 7.6 Hz), 4.06 (s, 3H), 3.29 (s, 2H). ^{13}C NMR (125 MHz, $CDCl_3$): δ 163.1, 134.7, 123.4, 116.3, 81.9, 79.2, 61.4. υ_{max} (thin film)/cm^{-1} 3289 (s), 2942 (w, br), 1463 (s), 1414 (s), 1251 (m), 1227 (m). MS-EI (*m/z*): 156[$M^{+\cdot}$], 141 [$M^{+\cdot}-CH_3$],126 [$M^{+\cdot}-OMe$]. HRMS-ESI (*m/z*): $[M+H]^+$ calcd for $C_{11}H_9O$ 157.0647; found 157.0645.

4.2.3. 2,6-Bis(bromoethynyl)anisole (17)

To 2,6-diethynyl anisole **16** (47 mg, 0.30 mmol) in acetone (15 mL) under argon was added *N*-bromosuccinimide (126 mg, 0.71 mmol), the reaction was then stirred for 3 h at rt, then diluted with H_2O (50 mL) and extracted with CH_2Cl_2 (3 × 30 mL). The combined organic extracts were washed with saturated $NaHCO_3$ (2 × 50 mL), dried ($MgSO_4$), filtered and concentrated in vacuo to give **17** as a pale brown solid (80 mg, 85%); mp 80–82 °C. Analytical samples were prepared by column chromatography on silica gel (25% EtOAc/Petroleum Spirits (40–60)). ^{1}H NMR (500 MHz, $CDCl_3$): δ 7.39 (d, 2H, J = 7.9 Hz), 6.98 (t, 1H, J = 7.9 Hz), 4.03 (s, 3H). ^{13}C NMR (125 MHz, $CDCl_3$): δ 163.1, 134.4, 123.3, 116.8, 75.6, 61.6, 54.2. υ_{max} (thin film)/cm^{-1} 2940 (w, br), 1462 (s), 1414 (s), 1236 (s), 1076 (m), 999 (s). MS-EI (*m/z*): 312, 314, 316 [$M^{+\cdot}$], 297, 299, 301[$M^{+\cdot}-CH_3$]. HRMS-ESI (*m/z*): $[M+H]^+$ calcd for $C_{11}H_7Br_2O$ 312.8858, 314.8843; found 312.8858, 314.8834.

4.2.4. Dimethyl 2,2′-(2-methoxy-1,3-phenylene)bis(2-oxoacetate) (18)

To 2,6-bis(bromoethynyl)anisole **17** (74 mg, 0.24 mmol) in MeOH (25 mL) was added a solution of $NaHCO_3$ (33 mg, 0.39 mmol) and $MgSO_4$ (233 mg, 0.94 mmol) in H_2O (14 mL). The reaction was cooled to 0 °C and stirred for 15 min, then $KMnO_4$ (149.8 mg, 0.95 mmol, 4 equiv) was added in portions over 1 h. The mixture was stirred for 1 h at 0 °C, then was diluted with H_2O (100 mL) and extracted with EtOAc (3 × 70 mL). The combined organic extracts were washed with brine (5 × 60 mL), dried ($MgSO_4$), filtered and concentrated in vacuo to give **18** as a clear oil (66 mg, 99%). ^{1}H NMR (500 MHz, $CDCl_3$): δ 8.07 (d, 2H, J = 7.6 Hz), 7.41 (t, 1H, J = 7.6 Hz), 3.94 (s, 6H), 3.79 (s, 3H). ^{13}C NMR (100 MHz, $CDCl_3$): δ 185.4, 164.0, 162.2, 136.8, 128.3, 124.8, 66.1, 52.9. υ_{max} (thin film)/cm^{-1} 3457 (w, br), 2957 (w), 2926 (w), 1732 (s, br), 1693 (s), 1683 (s), 1608 (m), 1463, (m), 1438 (m), 1421 (m), 1234 (s, br), 1151 (m), 1097 (m). MS-ESI (*m/z*): $[M+H]^+$ 281.1. HRMS-ESI (*m/z*): $[M+H]^+$ calcd for $C_{13}H_{13}O_7$ 281.0655; found 281.0654.

4.2.5. Dimethyl 2,2′-(2-hydroxy-1,3-phenylene)bis(2-oxoacetate) (19)

To a stirred solution of **18** (712 mg, 2.54 mmol) in DMF (20 mL) was added sodium ethanethiolate (372 mg, 4.42 mmol). The reaction was stirred for 3 h at 80 °C under nitrogen, then a further addition of sodium ethanethiolate (50 mg, 0.59 mmol) was added. The reaction was stirred overnight at 80 °C under nitrogen, then diluted with HCl solution (1 M, 100 mL) and extracted with CH_2Cl_2 (4 × 100 mL). The combined organic extracts were dried ($MgSO_4$), filtered and concentrated in vacuo. The crude yellow product (842 mg) was purified by chromatography on silica gel (50% EtOAc/Petroleum Spirit (40–60)) to give a yellow oil, which crystallized on standing to give **19** as pale yellow crystals (242 mg, 36% yield); mp 67–68 °C. ^{1}H NMR (400 MHz, $CDCl_3$): δ 12.01 (s, 1H), 8.15 (d, 2H, J = 8.0 Hz), 7.14 (t, 1H, J = 8.0 Hz), 3.99 (s, 6H).

^{13}C NMR (100 MHz, $CDCl_3$): δ 187.3, 163.7, 163.12, 138.9, 120.1, 120.0, 53.1. υ_{max} (thin film)/cm^{-1} 3087 (w, br), 2957 (w), 1739 (s), 1680 (m), 1645 (m), 1609 (m), 1584 (m), 1431 (m), 1318 (m, br), 1216 (s). HRMS-ESI (*m/z*): $[M+H]^+$ calcd for $C_{12}H_{11}O_7$ 267.0499; found 267.0499. HRMS-ESI (*m/z*): $[M-H]^-$ calcd for $C_{12}H_9O_7$ 265.0353; found 265.0350.

4.2.6. 2,2′-(2-Hydroxy-1,3-phenylene)bis(2-oxoacetic acid) (8)

To a solution of dimethyl 2,2′-(2-hydroxy-1,3-phenylene)bis(2-oxoacetate) **19** (10 mg, 37.5 μmol) in dioxane (2 mL) was added a solution of LiOH (6 mg, 0.25 mmol) in H_2O (1 mL). The reaction was stirred for 3 h then diluted with HCl solution (1 M, 20 mL) and extracted with EtOAc (3 × 10 mL). The combined organic extracts were dried ($MgSO_4$), filtered and concentrated in vacuo to give **8** as a pale brown oil (6.0 mg, 67%). ^{1}H NMR (500 MHz, $CDCl_3$): δ 12.03 (s, 1H), 8.45 (d, 2H, *J* = 8.0 Hz), 7.17 (t, 1H, *J* = 8.0 Hz). ^{13}C NMR (100 MHz, d_6-DMSO): δ 189.5, 165.4, 161.6, 137.7, 122.1, 119.5. υ_{max} (thin film)/cm^{-1} 2857 (w, br), 2512 (w, br), 1903 (w, br), 1672 (s, br), 1609 (s), 1475 (w), 1436 (s), 1279 (s), 1230 (s), 1184 (m), 1156 (m), 1023 (s), 972 (s, br), 764 (m), 668 (m). HRMS-ESI (*m/z*):$[M-H]^-$ calcd for $C_{10}H_5O_7$ 237.0040; found 237.0038.

4.2.7. Dimethyl 2,2′-(2-hydroxy-1,3-phenylene)bis-(2-(hydroxyimino)-acetate) (20)

To a solution of **19** (31 mg, 116 μmol) in dry MeOH (15 mL) was added hydroxylamine hydrochloride (33 mg, 474 μmol) and pyridine (2 drops). The reaction was stirred under nitrogen at rt overnight. Then the mixture was concentrated in vacuo and resuspended between HCl solution (1 M, 20 mL) and EtOAc (20 mL). The organic phase was separated and further washed with HCl solution (1 M, 2 × 10 mL), then dried ($MgSO_4$), filtered and concentrated in vacuo to give **20** as a brown oil (29 mg, 84% yield) as a 1:1 mixture of diastereomers (*Z,Z*):(*E,Z*). (*Z,Z*) *Diasteromer*: ^{1}H NMR (500 MHz, $CDCl_3$): δ 10.41 (s, 1H), 8.88 (br s, 2H), 7.36 (d, 2H, *J* = 7.8 Hz), 6.96 (t, 1H, *J* = 7.8 Hz), 3.95 (s, 6H). ^{13}C NMR (100 MHz, $CDCl_3$): 162.8, 155.8, 151.1, 131.0, 119.8, 117.4, 52.8. υ_{max} (thin film)/cm^{-1} 3328.8 (m, br), 3037.8 (w, br), 2956.9 (w), 1728.1 (s, br), 1603.0 (w, br), 1435.9 (m), 1323.3 (m, br), 1236.3 (s), 1177.7 (w), 1111.7 (m), 1091.9 (m), 997.1 (s), 910.4 (w), 840.2, (w), 731.2 (s).(*E,Z*) Diasteromer: ^{1}H NMR (500 MHz, $CDCl_3$): δ 10.28 (s, 1H), 8.92 (br s, 1H) 8.67 (br s, 1H), 7.36 (dd, 1H, J_1 = 7.5 Hz, J_2 = 2.0 Hz), 7.13 (dd, 1H, J_1 = 7.5 Hz, J_2 = 2.0 Hz), 6.99 (t, 1H, *J* = 7.5 Hz), 3.99 (s, 3H), 3.86 (s, 3H). ^{13}C NMR (125 MHz, $CDCl_3$): δ 163.9, 162.2, 154.8, 154.0, 148.2, 132.4, 130.1, 119.2, 118.2, 114.4, 53.1, 52.8. υ_{max} (thin film)/cm^{-1} 3328.4 (m, br), 2958.7 (w), 1733.5 (s, br), 1630.5 (w), 1604.7 (w), 1587.4 (w), 1436.9 (s), 1322.1 (m, br), 1239.7 (s), 1193.0 (w), 1177.2 (w), 1112.2 (s), 1091.3 (m), 1021.4 (m, br), 909.4 (w), 842.3 (w), 730.1 (s). MS-ESI (*m/z*): $[M+H]^+$ 297.27. HRMS-ESI (*m/z*): $[M-H]^-$ calcd for $C_{12}H_{11}N_2O_7$ 295.0571; found 295.0568.HRMS-ESI (*m/z*): $[M+Na]^+$ calcd for $C_{12}H_{11}N_2NaO_7$ 319.0536; found 319.0540.

4.3. Assay for monitoring DHDPS activity

UV–vis spectra and kinetic data were collected on either a Hewlett Packard 8452A Diode Array spectrophotometer with a circulating water bath to maintain a constant temperature of 30 °C or a Cary 50 Bio UV–vis Spectrophotometer equipped with a Haake P5/DC10 circulating water bath to maintain a constant temperature of 30 °C. The concentration of (*S*)-ASA was determined as previously described.[26] Modified assay conditions were utilized to determine rates of inactivation of phenolic inhibitors.[8,9] The concentration (activity) of DHDPS was optimised under control conditions (see below) to ensure an optimal rate where substrates would not limit the rate of reaction over the 2 min measurement. Control assays for initial screening and time dependent inhibition were conducted under standard modified assay conditions where DHDPS (810 μL, in HEPES, 200 mM pH 8.0, buffer) was incubated with DMSO (90 μL) prior to assay. Initial screening assays were conducted by incubating a solution of DHDPS (810 μL, in HEPES, 200 mM pH 8.0, buffer) with inhibitor (90 μL, made up in 100% DMSO) at a final concentration of 5 mM for 1 min prior to assay. Substrate protection experiments were conducted by incubating DHDPS with inhibitor and pyruvate (10 mM).

4.4. Analysis of enzyme kinetic data

Results were analysed by the methods of Copeland,[20,21] where the fractional velocities (υ_t/υ_0) of pre-incubated solutions of DHDPS at differing concentrations of inhibitor were determined. The observed decay curve for each concentration of inhibitor was fitted to Eq. I, to determine k_{obs}. A plot of k_{obs} versus [I] was fitted to Eqs. II, III, IV to determine values k_{off}, k_3, k_4, K_i^{app} and K_i^{*app} for slow-binding or slow-tight binding modes of inhibition (see Fig. 10 for description of k_{on}, k_{off}, k_3, k_4.

$$\frac{\upsilon_t}{\upsilon_0} = e^{(-k_{obs}\cdot t)} \quad \text{(I)}$$

Slow binding inhibition kinetics

$$k_{obs} = k_{off}\left(1 + \frac{[I]}{K_i^{app}}\right) \quad \text{(II)}$$

Slow-tight binding inhibition kinetics.

$$k_{obs} = k_4 + \left(\frac{k_3 \times [I]}{K_i^{app} + [I]}\right) \quad \text{(III)}$$

Slow-tight binding inhibition kinetics.

$$k_{obs} = k_4\left[\frac{1 + \frac{[I]}{K_i^{app}}}{1 + \frac{[I]}{K_i^{*app}}}\right] \quad \text{(IV)}$$

4.5. Mass spectrometry

All analyses were performed on an Agilent 6520 ESI-qTOF LC/MS Mass Spectrometer coupled to an Agilent 1100 LC system (Agilent, Palo Alto, CA). The instrument was operated in either positive or negative mode with: drying gas flow: 7 L min^{-1}, nebuliser: 30 psi, drying gas temp: 150–300 °C, Vcap: 3000–4000 V, Fragmentor: 25–215 V, Skimmer: 65 V, OCT RFV: 750 V. Scan range acquired: 100–3000 *m/z*. Mass spectra were deconvoluted using Agilent MassHunter Qualitative Analysis Build 3.0 software. DHDPS samples (10 μL) were incubated for either 10 min or overnight at rt with (1 μL) solutions of each respective inhibitor (made up in 100% DMSO)or control DMSO (1 μL) before injection into the ESI-qTOF.

$$\text{Slow} \quad E + I \underset{k_{off}}{\overset{k_{on}}{\rightleftharpoons}} EI$$

$$\text{Slow-tight} \quad E + I \underset{k_{off}}{\overset{k_{on}}{\rightleftharpoons}} EI \overset{k_3}{\underset{k_4}{\rightleftharpoons}} E^*I$$

Figure 10. Scheme of slow and slow-tight binding inhibition showing initial on/off rates to form EI complex, with slow-tight enzyme isomerization k_3 to form $E*I$ complex with slow reverse rate k_4.

Acknowledgments

This work was supported by the Defense Threat Reduction Agency (Project ID AB07CBT004) (C.A.H.) and the Royal Society of New Zealand Marsden Fund (J.A.G. and C.A.H.). The authors thank R.C.J. Dobson, S.R.A. Devenish, F.G. Pearce, S. Dommaraju and M.A. Perugini for providing samples of DHDPS and DHDPR used in enzyme assays, and for useful discussions.

Supplementary data

Supplementary data associated with this article can be found, in the online version, at doi:10.1016/j.bmc.2012.01.045.

References and notes

1. Bukhari, A. I.; Taylor, A. L. *J. Bacteriol.* **1971**, *105*, 844.
2. Pavelka, M. S., Jr.; Jacobs, W. R., Jr. *J. Bacteriol.* **1996**, *178*, 6496.
3. Hutton, C. A.; Perugini, M. A.; Gerrard, J. A. *Mol. BioSys.* **2007**, *3*, 458.
4. Hutton, C. A.; Southwood, T. J.; Turner, J. J. *Mini-Rev. Med. Chem.* **2003**, *3*, 115.
5. Cox, R. J.; Sutherland, A.; Vederas, J. C. *Bioorg. Med. Chem.* **2000**, *8*, 843.
6. Cox, R. J. *Nat. Prod. Rep.* **1996**, *13*, 29.
7. Shedlarski, J. G.; Gilvarg, C. *J. Biol. Chem.* **1970**, *245*, 1362.
8. Boughton, B. A.; Dobson, R. C. J.; Gerrard, J. A.; Hutton, C. A. *Bioorg. Med. Chem. Lett.* **2008**, *18*, 460.
9. Boughton, B. A.; Griffin, M. D.; O'Donnell, P. A.; Dobson, R. C.; Perugini, M. A.; Gerrard, J. A.; Hutton, C. A. *Bioorg. Med. Chem.* **2008**, *16*, 9975.
10. Blickling, S.; Renner, C.; Laber, B.; Pohlenz, H.-D.; Holak, T. A.; Huber, R. *Biochemistry* **1997**, *36*, 24.
11. Structure provided through private correspondence with R. Huber.
12. Li, L.-S.; Wu, Y.-L. *Tetrahedron Lett.* **2002**, *43*, 2427.
13. Liu, K.-G.; Hu, S.-G.; Wu, Y.; Yao, Z.-J.; Wu, Y.-L. *J. Chem. Soc., Perkin Trans. 1* **2002**, 1890.
14. Chimenti, F.; Bolasco, A.; Secci, D.; Chimenti, P.; Granese, A. *Synth. Commun.* **2004**, *34*, 2549.
15. Villeneuve, K.; Riddell, N.; Jordan, R. W.; Tsui, G. C.; Tam, W. *Org. Lett.* **2004**, *6*, 4543.
16. Dodge, J. A.; Stocksdale, M. G.; Fahey, K. J.; Jones, C. D. *J. Org. Chem.* **1995**, *60*, 739.
17. Feutrill, G. I.; Mirrington, R. N. *Tetrahedron Lett.* **1970**, 1327.
18. Feutrill, G. I.; Mirrington, R. N. *Aust. J. Chem.* **1972**, *25*, 1719.
19. Feutrill, G. I.; Mirrington, R. N. *Aust. J. Chem.* **1972**, *25*, 1731.
20. Copeland, R. A. *Enzymes: A Practical Introduction to Structure, Mechanism, and Data Analysis*, 2nd ed.; Wiley-VCH, Inc, 2000.
21. Copeland, R. A. *Evaluation of Enzyme Inhibitors in Drug Discovery—A Guide for Medicinal Chemists and Pharmacologists*; Wiley-VCH, Inc, 2005.
22. Alexeev, D.; Baxter, R. L.; Campopiano, D. J.; Kerbarh, O.; Sawyer, L.; Tomczyk, N.; Watt, R.; Webster, S. P. *Org. Biomol. Chem.* **2006**, *4*, 1209.
23. Aldini, G.; Granata, P.; Carini, M. *J. Mass Spectrom.* **2002**, *37*, 1219.
24. Yeboah, F. K.; Alli, I.; Yaylayan, V. A.; Konishi, Y.; Stefanowicz, P. *J. Agric. Food Chem.* **2000**, *48*, 2766.
25. Borthwick, E. B.; Connell, S. J.; Tudor, D. W.; Robins, D. J.; Shneier, A.; Abell, C.; Coggins, J. R. *Biochem. J.* **1995**, *305*, 521.
26. Coulter, C. V.; Gerrard, J. A.; Kraunsoe, J. A. E.; Pratt, A. J. *Pestic. Sci.* **1999**, *55*, 887.